

Green synthesized 3D Coconut Shell Biochar/Polyethylene Glycol Composite as Thermal Energy Storage Material

B Kalidasan ^a, AK Pandey ^{a,b*}, R Saidur ^{a,c}, Belqasem Aljafari ^d, Aman Yadav ^e, M Samykano ^e

^{a)} *Research Centre for Nano-Materials and Energy Technology (RCNMET), School of Engineering and Technology, Sunway University, No. 5, Jalan Universiti, Bandar Sunway, Petaling Jaya, 47500 Selangor Darul Ehsan, Malaysia*

^{b)} *Center for Transdisciplinary Research (CFTR), Saveetha Institute of Medical and Technical Sciences, Saveetha University, Chennai, India*

^{c)} *Lancaster University, Lancaster LA1 4YW, United Kingdom*

^{d)} *Electrical Engineering Department, College of Engineering, Najran University, Najran, 11001, Saudi Arabia*

^{e)} *Faculty of Mechanical & Automotive Engineering Technology, University Malaysia Pahang Al-Sultan Abdullah, 26600 Pekan, Pahang, Malaysia*

Abstract

Developing stable, economic, safer and carbon-based nanoparticles from agro solid waste facilitates a new dimension of advancement for eco-friendly nanomaterials in competition to existing nanoparticles. Herewith, a three dimensional highly porous honeycomb structured carbon-based coconut shell (CS) nanoparticle is prepared through green synthesis technique using tube furnace to energies organic phase change material (PCM). CS nanoparticle synthesis using a green approach is incorporated with polyethylene glycol (PEG) using a two-step technique to develop PEG/CS nanocomposite PCM. Thermophysical features of the nanocomposites are characterized using transient hot bridge (ThB), differential scanning calorimeter (DSC) and thermogravimetric analysis (TGA), whereas optical property and chemical stability is evaluated using UV-Vis and FTIR spectrometers. Resulting nanocomposite demonstrates higher thermal conductivity by 114.5% (improved from 0.24 W/m·K to 0.515 W/m·K). Energy storage enthalpy increased from 141.2 J/g to 150.1 J/g with 1.0% weight fraction of CS nanoparticles. Optical absorbance of the nanocomposite is improved by 2.14 times compared to base PCM. The developed nanocomposite samples exhibit extreme thermal stability up to 215 °C. The 3D porous structure of CS nanoparticles shows better contact area with PEG, causing low interfacial thermal resistance for improved thermal network channels and pathways for extra heat transfer and phonon propagation.

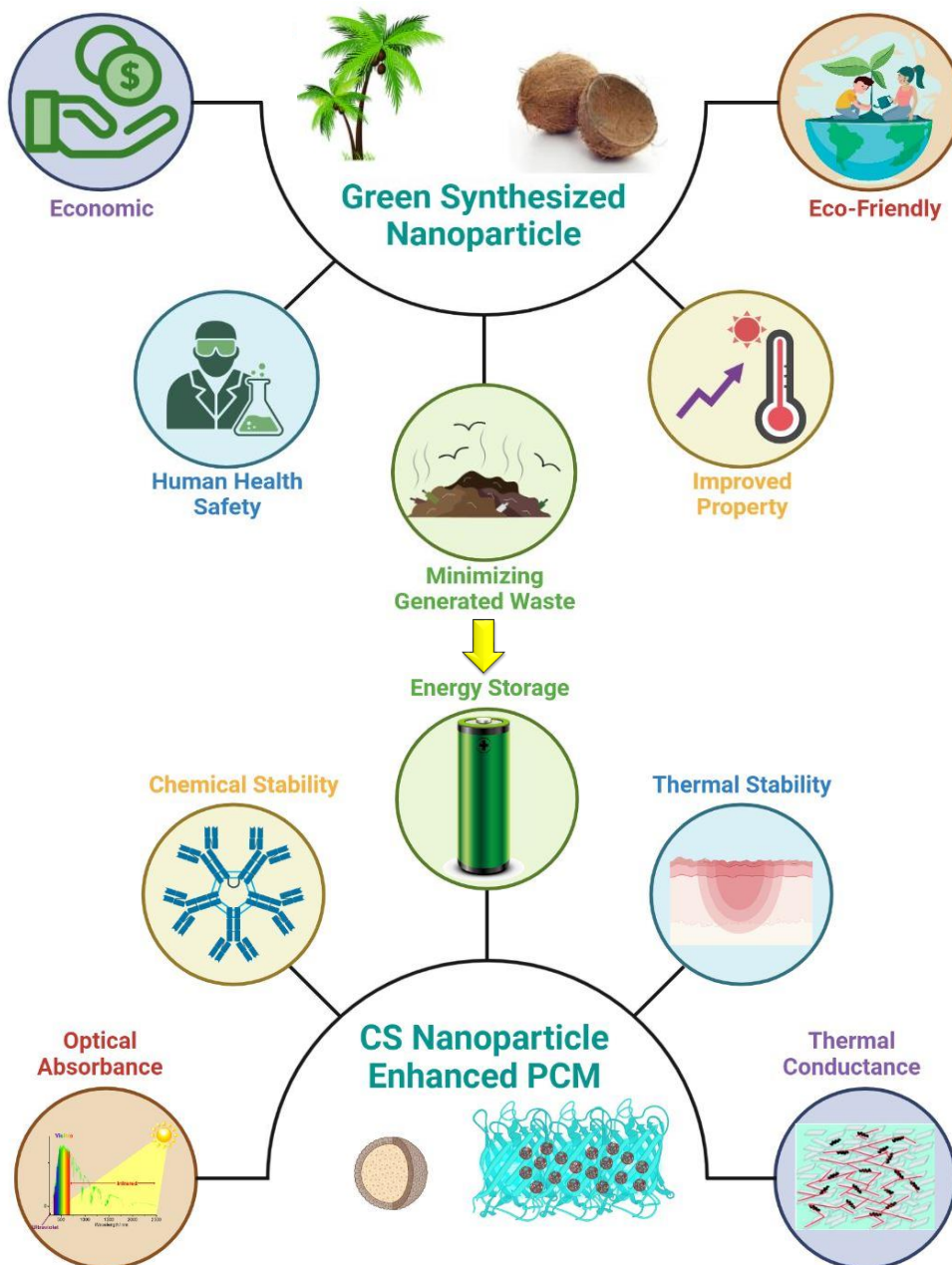
Keywords: Coconut Shell; Green Synthesise; 3D Nanoparticle; Phase Change Material; Thermal Energy Storage;

*Corresponding author: adarshp@sunway.edu.my (AK Pandey)

35 **Highlight**

- 36 • Green synthesised 3Dimensional, highly porous carbon-based nanoparticle
- 37 • Up to 114.5% thermal conductivity improvement with CS nanoparticle
- 38 • Increase in latent heat capacity (6.3%) from 141.2 J/g to 150.1 J/g
- 39 • Optical absorbance increases more than 2 folds and transmissibility falls by 69%
- 40 • Excellent thermal cycle stability for 500 thermal cycles.

41 **Graphical Abstract**



42

43

44 1.0 Introduction

45 Application of phase change materials (PCMs) as an energy storage technology can improve
46 the efficiency of energy utilisation through the phase transition process, which is a cost effective
47 passive technology [1]. Generally, PCM are of three types a) Organic (fatty acid, sugar alcohol,
48 paraffin); b) Inorganic (salt hydrate); c) Eutectic (blend of organic & inorganic) [2]. Organic PCMs
49 are predominantly preferred as thermal energy storage materials over inorganic PCM owing to their
50 ability to store energy at wide range of temperature, high heat storage density [3], better chemical &
51 thermal stability [4], isothermal behaviour, no issue of supercooling [5], non-corrosive in nature [6],
52 eco-friendly and economical. **Despite numerous advantages of PCM, most of the organic PCM lack
53 thermal conductivity, poor optical absorbance and leakage issue; which limits their applications for
54 many thermal regulation solutions.** Nonetheless, to improve the thermal characteristics of organic
55 PCM, different dimensional nanoparticles like carbon nanotubes [7], graphene [8], expanded
56 graphite, hybrid conducting polymers [9] and tetrapods [10] has been explored. **In majority of the
57 case the optical absorbance of organic PCM matrix are enhanced by the nanomaterials dispersed with
58 PCM to enhance the thermo-physical characteristics. Likewise, to overcome leakage issue core PCM
59 are encapsulated using silica gel [11]; as well shape stabilized via wood powder/high density
60 polyethylene [12].** However, all the aforementioned nanomaterials continue to confront challenges
61 with high manufacturing costs and difficulty in mass production, resulting in the development of
62 most nanomaterials remaining at the laboratory stage, making large-scale manufacture and use
63 challenging. In addition, these nanoparticles are toxic and costlier. After usage, these nanoparticles
64 are eventually dispersed into the environment, henceforth there is an utmost need for eco-friendly
65 nanoparticle.

66 Green synthesis of biochar nanoparticle is an emerging eco-friendly technology adopted in
67 converting solid waste (e.g. manure, corn cub, rice husk, eggshell, bamboo) and industrial waste (e.g.
68 waste tyre, sawdust) into nanoparticle. The nanoparticles synthesised via green technology contain
69 more functional groups of C–O and C=O rather than activated carbon. A derivative of charcoal, and
70 activated carbon holds the merit of large specific surface area, chemical stability, ample availability
71 and low density [13]. Nevertheless, usage of activated carbon suffers owing to a) non-renewable
72 nature; b) higher cost and c) difficult to regenerate [14]. Whereas, biochar is an emerging
73 environmentally friendly safer material; and can be prepared from agro & forest residues [15]. Other
74 benefits of green synthesised biochar carbon nanoparticle includes a) cheaper; b) renewable; c) ease
75 of preparation; d) large sorption potential; e) protect environment as can be developed from waste;
76 e) high surface area [16]; f) 3D porous structural framework; g) superior resistance to corrosion and
77 heat and h) higher thermal and electrical conductance [17]. Henceforth, numerous research works on

78 biochar preparation and their utilisation with energy storage domains were explored. Sheng et al. [18]
79 dispersed biochar derived from sisal fibre (1D carbon bundles) with paraffin to enhance the thermal
80 conductivity from 0.25 W/m·K to 1.73 W/m·K at carbon ratio of 12.8%. Significant improvement in
81 thermal conductivity of the composite was attributed by the anisotropic one dimensional arrangement
82 of sisal fibres exhibited better thermal networks. Likewise, Das et al. [19] dispersed biochar of water
83 hyacinth (PCM: biochar of 4:6; 5:5; 6:4; 7:3; 8:2; 9:1 wt%) to develop form stable PCM with
84 improved thermal conductivity of composite PCM by 13.8 times (PCM: biochar of 6:4 wt%).
85 Conversely, Xiong et al. [20] green synthesised biochar nanoparticles using garlic stem and dispersed
86 the developed nanoparticle with paraffin at a weight fraction of 1wt%, 3wt% and 5wt%. Owing to
87 the two dimensional flake structure of garlic stem nanoparticle and thermally conductive networks
88 within the matrix of paraffin PCM, the thermal conductance improved from 0.19 W/m·K to 0.24
89 W/m·K with 5% weight fraction of garlic stem nanoparticle. Similarly Lv et al. [21] experimentally
90 investigated the thermal performance of a variety of PCM like paraffin, stearic acid and PEG using
91 biochar developed from phoenix leaf. The PCM:biochar proportion was 75:25 wt%. Interestingly,
92 results depicted that biochar pyrolyzed at higher temperature caused higher graphitization and
93 increased the thermal conductivity of nanocomposites, rather than the biochar nanoparticle pyrolyzed
94 at lower temperature. Conversely, Wan et al. [22] prepared a form stable PCM using palmitic acid
95 and biochar of pinecone at different mass ratios of 4:7, 4:6, 5:5, 6:4 and 6.5:3.5. Increase in thermal
96 conductivity for palmitic acid: biochar of pinecone at 6:4 was about 43.76% as palmitic acid was
97 impregnated within the pores of pinecone biochar resulting in better thermal network channels. Pinus
98 resinosa fruit was pyrolyzed to develop biochar with high porosity and surface area by Mandal et al.
99 [23]. Developed biochar was dispersed with dodecanoic acid to fabricate a shape stabilised composite
100 PCM to overcome the issue of leakage with 3:1 proportion of dodecanoic acid to biochar. Hybrid of
101 graphene oxide and biochar corn straw was developed into nanoparticle to improve the thermal
102 conductivity and shape stability of polyethylene glycol operating at 410 °C [24]. Similarly Atinafu
103 et al. [25] developed hybrid nanoparticle with a mixture of carbon nanotube and biochar of bamboo
104 via hydrothermal method. Above synthesised nanoparticle was dispersed with liquid dodecane to
105 prepare a thermally interconnected heat transfer composite PCM with leak proof and improved
106 thermal conductivity. Goud et al. [26] developed a shape stable PCM for thermal regulation of lithium
107 ion batteries. In his research work, authors opted myristyl alcohol as PCM and enhanced its
108 performance with biochar derived from neem tree as supporting material, in addition the thermal
109 conductivity of the composite increased by 3.91 times at a weight fraction of 24%. Bordoloi et al.
110 [27] developed biochar using a) yellow oleander; b) water hyacinth and c) sugarcane bagasse to be
111 used as supporting matrix to overcome the issue of low thermal conductance and issue of leakage in

112 commercialised organic PCM. Thermal conductivity of the composite increased from 0.126 W/m·K
113 to 0.154 W/m·K with a mixture of biochar developed from all three sources of biomass owing to the
114 heat conductance carbon networks of the dispersed biochar. Based on the literature studies discussed
115 above and best of author's knowledge, a gap is identified in exploring the potential of green
116 synthesised biochar of coconut shell to opt as nanomaterial. Whereas in the current research we
117 perform carbonising in a control atmosphere ensuring pollution free synthesis technique.
118 Furthermore, there is an utmost attraction towards synthesis of eco-friendly nanomaterials
119 demonstrating effective thermo-physical characteristics to compete with the commercial
120 nanomaterials.

121 Herein, we synthesise a new carbon-based nanoparticle by carbonization of coconut shell
122 (CS) adopting a green synthesise technique for contemporaneously providing enhanced thermal
123 conducting features and optical absorbance of organic PCM. Coconut (Scientific name: *Cocos*
124 *Nucifera*) shell was opted as a precursor for carbon based nanoparticle developed owing to a) eco-
125 friendly, low cost agro based solid waste; b) can be transferred into activated biochar through
126 carbonization process with high carbon content; c) exhibit higher surface area to volume, with porous
127 nature and thermal conductive [28]; d) can be readily procured as India accounts for 31.45% of world
128 coconut production and leads globally according to data from Indian Trade Portal and Malaysia is
129 ranked as the 12th largest producer of coconut. Polyethylene glycol (PEG) operating at phase
130 transition temperature of 35-38°C with 142 J/g of latent heat storage has been selected owing to their
131 special feature of non-corrosiveness; no degree of supercooling; economical; chemically stable and
132 best preferred for thermal regulation units. Nonetheless, the issue of low thermal conductivity and
133 poor optical absorbance confines real time application of PEG in most of the thermal energy storage
134 and thermal regulation implementations. Ultimately there is a need for energising nanoparticles with
135 features of being sustainable, cheaper, non-reactive, non-toxic, non-polluting, highly stable, available
136 in nature and easy to handle. [Table 1 compares a few recent studies that used biochar-based
137 nanoparticles to improve the heat transfer characteristics of PCM in comparison with the present
138 research. To the best of the author's knowledge and the literature studies in table 1, there is a need for
139 additional studies into the possibility of using green biochar made from coconut shells as a
140 nanomaterial. Exploring the potential of coconut shell as nanoparticle via green synthesis technique
141 to enhanced the thermo physical characteristics of organic PCMs and energy storage materials would
142 be of great scientific benefit. Additionally, coconut shells are a naturally occurring agricultural
143 resource that is used as a cooking fuel in rural areas despite being considered a waste product. CS
144 nanoparticle are easy for mass production at low cost, and are significant for effective
145 commercialisation. In contrast, the current study uses a synthesis process that ensures no pollution](#)

146 by carbonising in a control atmosphere. In order to compete with commercial nanomaterials, there is
147 also a strong pull towards the synthesis of eco-friendly nanomaterials with strong thermo-physical
148 properties. Henceforth, in this research framework we develop PEG/CS nanocomposite PCM
149 operating at phase transition temperature of 35-38 °C with different weight fraction (0.3 wt%, 0.5
150 wt%, 0.7 wt%, 1.0 wt% & 1.3 wt%) of CS nanoparticle via two step method. Morphological
151 behaviour, chemical stability of functional group, optical property (absorbance & transmissibility),
152 energy storage potential (heating & cooling), thermal conductivity, degradation stability, reusable
153 reliability and thermal performance of PEG/CS nanocomposite is experimentally tested and analysed.
154 Thermal reliability of the developed nanocomposite PCM is evaluate for 500 number of thermal
155 cycles. Results and findings ensure the potential of green synthesised carbon based CS nanoparticles
156 in energising organic PCM. Influence of porous nature, non-uniform structure and 500-800 nm sized
157 CS NP causing low interfacial thermal resistance for improved thermal network channels and
158 pathways for extra heat transfer and phonon propagation are discussed. Conversely, PEG blends
159 within the micro pores of CS nanoparticles and between lamellar structures for ensuring better energy
160 storage is explained. Developed PEG/CS nanocomposite are less dense and economical for thermal
161 regulation applications with more focus on sustainable future. Based on experimentally determined
162 thermal characteristics the developed organic nanocomposite PCM is expected to contribute
163 effectively for thermal regulation units with more focus on sustainability.

164 *Table 1: Biochar nanoparticle for enhanced thermal features of phase change materials*

Nano material	PCM Ratio (%)	Thermal Conductivity (%)	Energy Storage (J/g)		Reference
			ΔH_m	ΔH_c	
Expanded Perlite	70.1	-38.78	-23.64	-22.13	[29]
Expanded Perlite/Carbon	66.4	82.12	-29.01	-26.70	
Diatomite	50	10.34	-39.01	-50.68	[30]
Diatomite/Expanded Graphite	47.5	68.96	-42.84	-52.15	
Diatomite/Expanded Graphite	45	131	-44.36	-54.28	
Expanded Vermiculite	66.1	-	-33.93	-33.90	[31]
Expanded Vermiculite/Silver nanowire	62.1	104	-37.87	-37.91	

Hybrid (Corn Straw + Graphene Oxide)	80	3.7	-34.1	-32.1	[24]
	95	1592	-8.5	-7.8	
Graphene Nanosheets	90	2592	-12.6	-14.1	[32]
	85	4707	-16.8	-17.8	
MWCNTs	99.5	37	+6.1	+3.1	[33]
Reduced Graphene Oxide	98	-	-4.67	-7.9	[34]
Coconut Shell Nanoparticle	99	114.58	+6.30	+2.46	This work

165

166 2.0 Materials and Methods

167 2.1 Materials

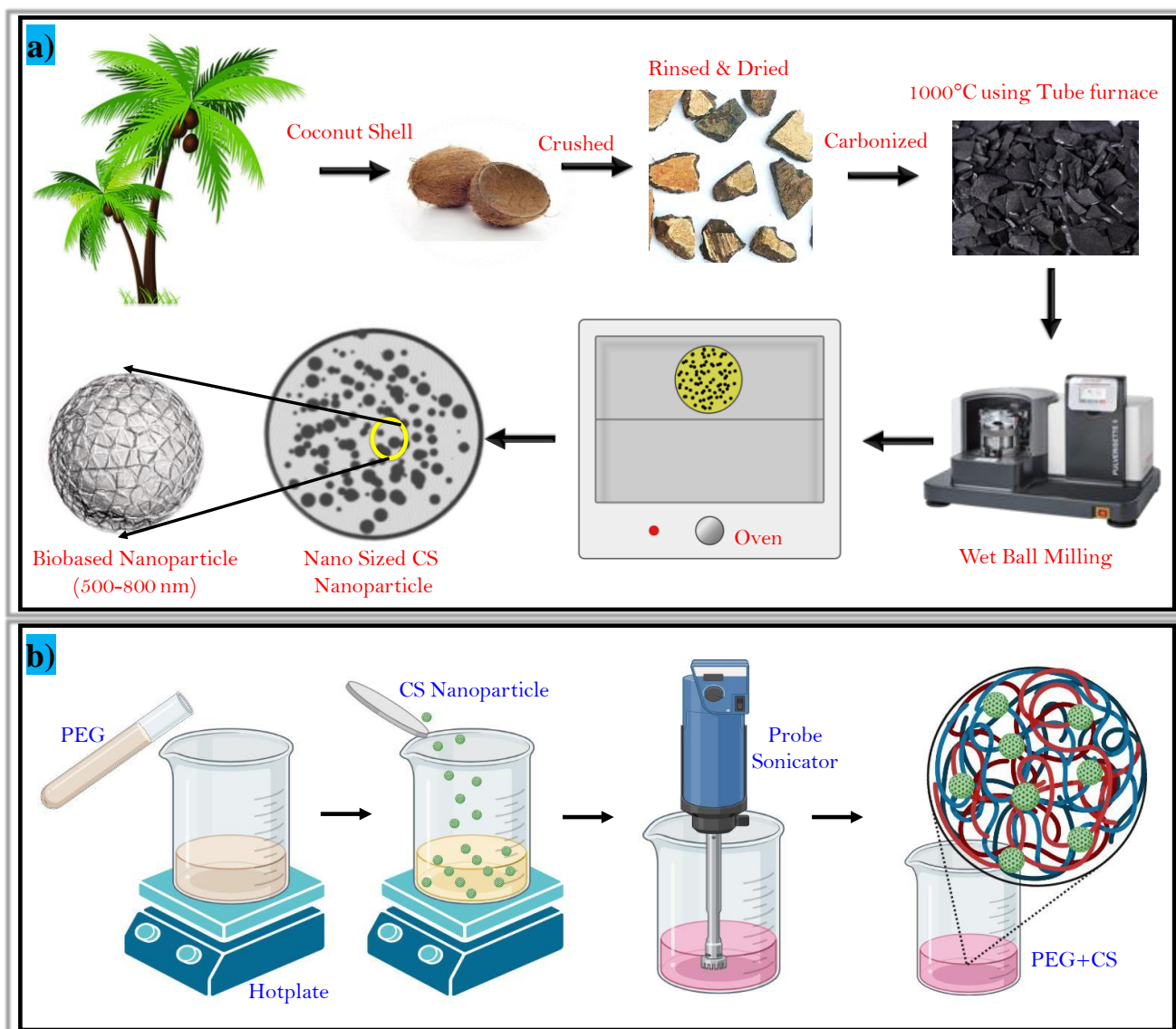
168 Energy storage material opted in the current research work is polyethylene glycol (PEG-1000)
169 with a phase transition temperature of 35-38 °C, acquired from Millipore Sigma. PEG-1000 has a
170 melting enthalpy of 146 J/g, density of 1.2 g/cm³ with white colour appearance. Agro solid waste of
171 coconut shell (CS) was acquired from Tamil Nadu, India which is used as the raw waste material for
172 the green synthesis of CS nanoparticles. The green synthesise technique adopted for preparing the
173 nanoparticle developed in the current research investigation is described in Section 2.2.

174 2.2 Synthesis of Coconut Shell Biochar based Nanomaterial

175 This section describes the green synthesis technique adopted to develop coconut shells into
176 useful nanoparticles for effective energy storage materials. Figure 1a provides pictorial representation
177 of techniques involved in green synthesis of nanomaterial from solid waste. To begin with, coconut
178 shells are extracted from agro solid waste and smashed into smaller pieces of size 20-25 mm using
179 mallet. We wash the coconut shell using deionized water to remove dust and sand particles to develop
180 nanoparticles of better features. Followed by washing, the cleaned coconut shells are dried in vacuum
181 over 125 °C for 12 hours. Furthermore, coconut shells are converted into biochar by the carbonisation
182 process. Coconut shell is carbonised in a nitrogen atmosphere at a temperature of 1000 °C using a
183 high temperature tube furnace ensuring pollution free technique. The carbonised coconut shell scraps
184 are further processed using hand crushing and wet ball milling to reduce their particle size. Using
185 hand crushing, the carbon scraps of coconut shells are reduced to 1.5-1.8 µm, tailed by wet ball
186 milling for 24 hours at 500 rpm with dwell period of 05 minutes in between every 10 minutes of
187 operation. Wet ball milling is carried out using 1 mm balls to particulate the carbon coconut shell

188 scraps with inclusion of water. The ball milled samples are dried in an oven at 200 °C to obtain the
189 final nanoparticle.

190 To explore the size and elemental composition of the green synthesis CS nanoparticle, the
191 developed nanoparticle is tested using particle sizer and Energy Dispersive X-Ray Analysis (EDX).
192 Particle size indicates the size of the CS nanoparticle to be in the range of 500-800 nm. The
193 synthesised nanoparticle comprised of 92% of carbon element as evaluated under EDX and also
194 indicates the presence of other elements like O, K, Cl, Ca, Si, Na and Al as can be inferred from
195 **(Supplementary S2-S3 and T2- Appendix III)**



196
197 *Figure 01: a) Green synthesis process of coconut shell into nanomaterial; b) Step by step*
198 *development process of CS nanoparticle dispersed organic PCM.*

199 **2.3 Preparation of Coconut Shell Biochar/Polyethylene Glycol Composite**

200 In the current experimental investigation, CS biochar nanoparticle synthesised as described
201 in section 2.2 is dispersed with organic PCM PEG-1000 to develop the nanocomposite adopting a

202 two-step technique. Figure 1b illustrates the preparation technique of CS nanoparticle dispersed PEG-
203 1000 nanocomposite. Initially, 20 g of PEG-1000 is weighed and melted in a beaker using a hot plate
204 maintained at 65°C. Subsequently, we disperse 0.04 g (0.2%) of the green synthesised CS
205 nanomaterial with PEG-1000 PCM melted to liquid state. The nanocomposite mix is now sonicated
206 using a probe sonicator for 45 minutes and the nanocomposite is cooled down to obtain the required
207 green synthesised CS biochar based nanoparticle dispersed PCM nanocomposite sample. The
208 developed PEG+CS biochar nanoparticles are considered for further morphological, chemical,
209 optical and thermal characterization evaluations. Likewise, to determine the optimum weight
210 concentration of CS nanoparticles exhibiting the improved thermal feature, nanocomposite samples
211 are developed with weight fraction of 0.3%, 0.5%, 0.7%, 1.0% and 1.3% CS nanomaterial.

212 **2.4 Characterization Techniques and Instruments**

213 To synthesise the nanoparticle, develop the nanocomposite, characterise the morphological
214 behaviour, exhibit the thermo physical properties and to evaluate the thermal cycling ability of PEG-
215 1000 with CS nanoparticle we opt for a few sensitive instruments. We use a high temperature tube
216 furnace (Model: Gero 30-3000 °C, Carbolite) for carbonising the coconut shell into biochar in an
217 eco-friendly manner. Planetary ball mill (Model Pulverisette 5, Fritsch, Germany) is used to reduce
218 the green synthesised biochar into finer nanoparticles. Particle size of the synthesised CS nanoparticle
219 using particle analyser by Anton Paar (Model: Litesizer 500). The FESEM instrument was fortified
220 with an Energy Dispersive X-ray Spectroscopy (Oxford Instrument EDX) system, which was
221 operated to determine the elemental compositions of the PCM composite samples. To analyse the
222 chemical stability of the CS based nanocomposite PCM Fourier Transform Infrared Spectroscopy
223 (FTIR) (Model: FTIR Spectrum TWO, Perkin Elmer) is used. Thermal conductivity is determined
224 using TEMPOS with dual needle SH-3, at room temperature of 25 °C. Differential scanning
225 calorimetry (DSC) (Model: DSC 3500 Sirius, NETZSCH) was used to analyse the melting
226 temperature and latent heat properties of PCM composite. DSC melting and cooling curves were
227 inspected between 05 °C and 55 °C under the N₂ atmosphere with a heating rate of 5 °C/min. A
228 thermogravimetric analyzer (TGA) (Model: TGA 4000, Perkin Elmer) is used to conduct a thermal
229 deterioration analysis on pure PCM and the composite PCM. The temperature for TGA is ramped up
230 to 500 °C at a rate of 10 °C/min in an N₂ environment. A customized thermal cycling unit is used to
231 accelerate the charging and discharging cycle of the developed nanocomposite. The uncertainty
232 associated with the instruments are provided ([Supplementary T1- Appendix D](#)). All curves were
233 plotted in Origin software.

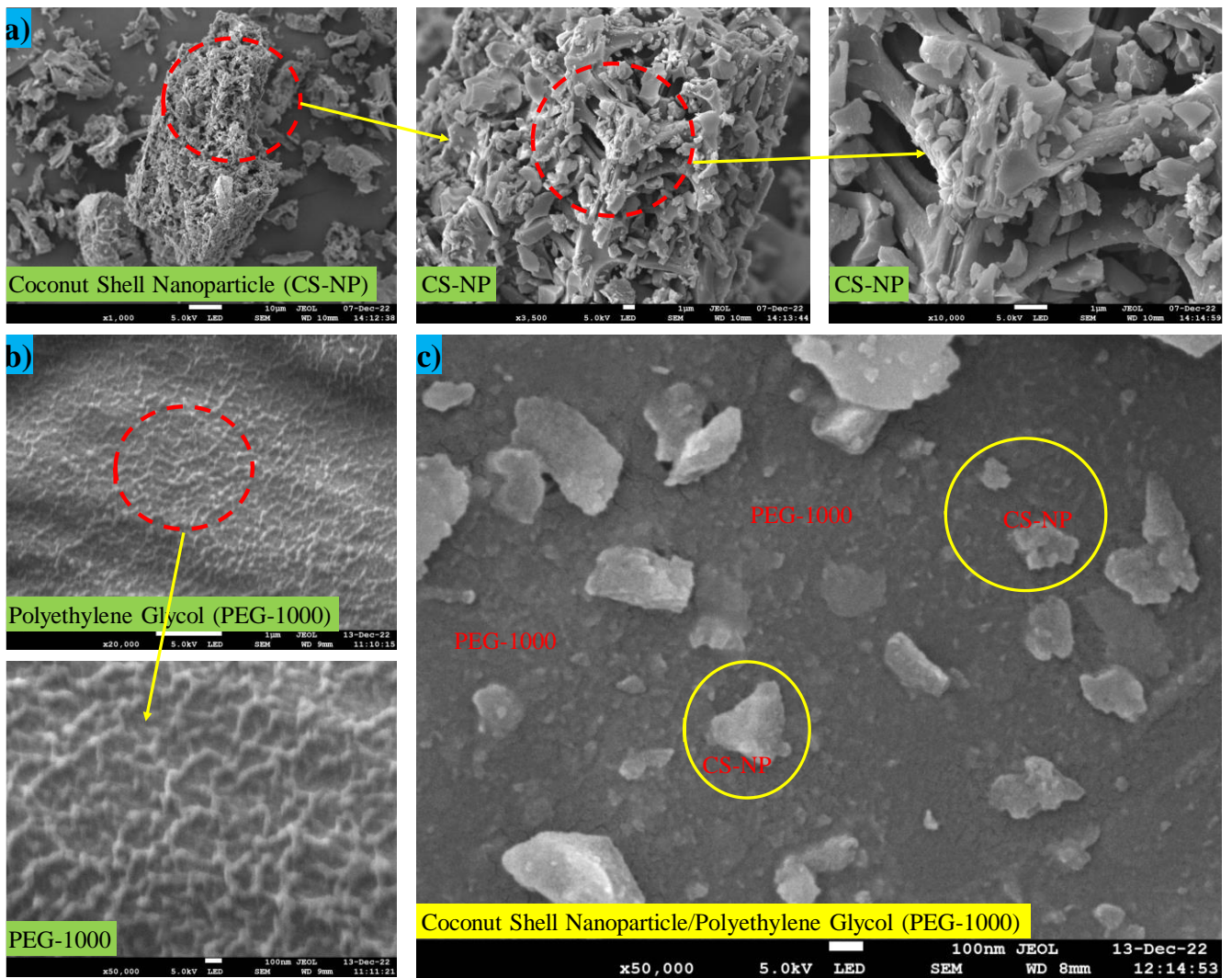
234

235 **3.0 Results and Discussion**

236 The current research work is focused on synthesising of eco-friendly nanoparticles in a
237 greener way to enhance the chemical, thermal and optical features of organic PCM. This section
238 illustrates and scientifically discusses the special features of coconut shell nanoparticles for
239 energising the polyethylene glycol PCM. Morphological behaviours, chemical stability, energy
240 storage potential, thermal conductivity, optical absorbance and transmittance of electromagnetic
241 spectrum and thermal stability of CS nanoparticle dispersed composite PCMs are discussed below.

242 **3.1 Microstructure and morphological visuals**

243 To understand the microstructure, morphology and interaction of the synthesised CS
244 nanoparticle, polyethylene glycol PCM and the nanocomposite of CS nanoparticle and phase change
245 materials, SEM are presented in Figure 2. To begin with, the morphological and microstructure of
246 the green synthesised CS nanoparticle is presented. The CS nanoparticle used in the current research
247 to enhance the thermal feature of PEG-1000 PCM is green synthesised using agro waste of coconut
248 shell. Figure 2a on a microscopic level displays the three dimensional multiple layered hollow
249 structure (contributing to higher specific surface area) portraying a honeycomb shape, with numerous
250 porous holes. The characteristic of high porosity and greater specific surface area of CS nanoparticles
251 may facilitate in sustaining organic PEG PCM and safeguard resistance to leakage in molten state
252 [when included in higher proportion \(20%\) owing to better surface tension and capillary action \(A](#)
253 [form stable nanocomposite with PEG+CS-20% is evaluated for form stability in Supplementary S1,](#)
254 [Appendix II\)](#). Owing to higher surface area compared to the volume, CS nanoparticles exhibit the
255 ability to adsorb higher capacity of liquid molecules during phase transition of organic PCM, and
256 supports stable PCM operating at lower temperature [35]. Figure 2b, represents the sticky nature with
257 wavy surface of PEG-1000 organic PCM belonging to the family of alkane with long chains of
258 polymer. Morphological visuals of CS dispersed PEG-1000 nanocomposite samples are presented in
259 Figure 2c. We observe a uniform dispersion of CS nanoparticles over the PEG matrix, without any
260 agglomeration and clustering. PEG blends within the micro pores of CS nanoparticles and between
261 lamellar structures and ensures better energy storage to occur. The uniformly distributed CS
262 nanoparticle establishes thermal hotspots within the PEG matrix and contributes in enhancing the
263 heat transfer rate. Additionally the elemental analysis of PEG and PEG-BNP nanocomposites
264 samples are presented in the supplementary document for further exploration ([Supplementary S4-](#)
265 [S7 and T3-T4, Appendix III\)](#).

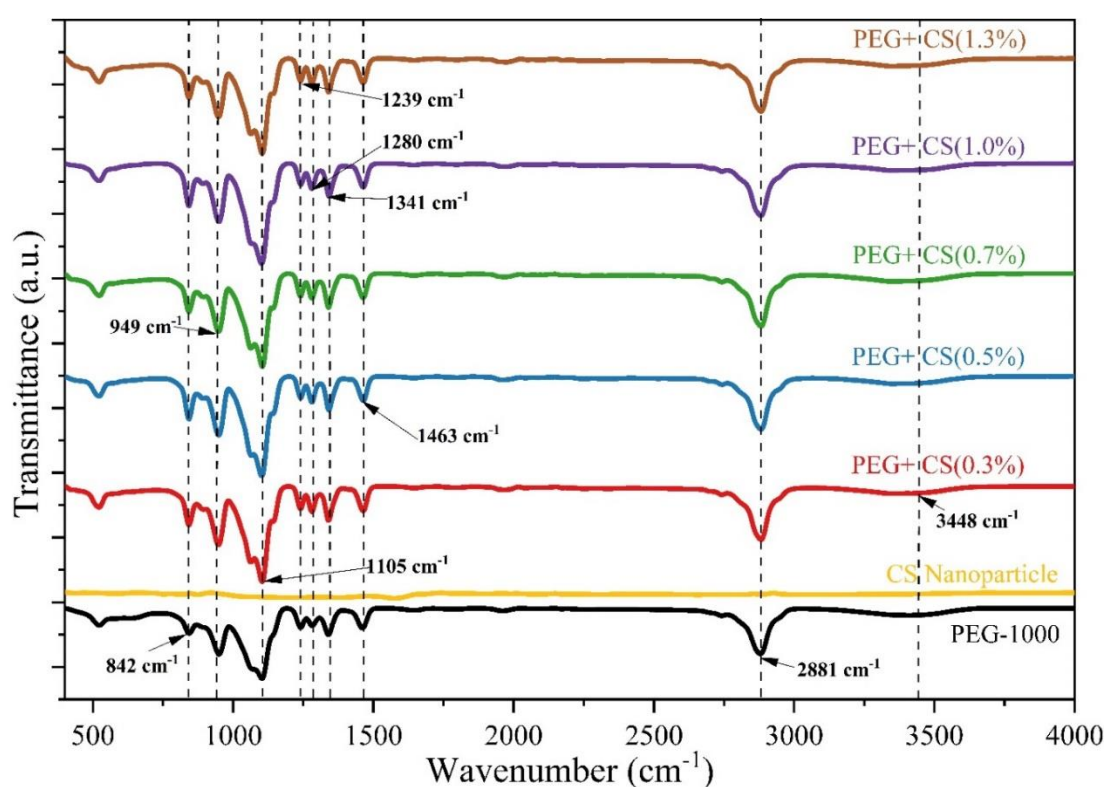


266
 267 *Figure 2: Microstructure of a) Coconut shell biochar; b) PEG-1000 and c) Coconut shell biochar*
 268 *dispersed PEG-1000 PCM.*

269 3.2 Chemical stability evaluation using FTIR

270 The chemical stability and compatibility between PEG-1000 PCM and the green synthesised
 271 CS nanoparticle was experimentally investigated using the FTIR spectrometer, and the spectral peaks
 272 corresponding to each wavenumber are presented in Figure 3. Spectral peaks of PEG-1000, CS
 273 nanoparticle and nanocomposite samples of CS nanoparticle dispersed PEG-1000 are investigated.
 274 In pure PEG-1000 PCM the absorption bands occurred at 842 cm^{-1} , 949 cm^{-1} , 1105 cm^{-1} , 1239 cm^{-1} ,
 275 1280 cm^{-1} , 1341 cm^{-1} , 2880 cm^{-1} and 3450 cm^{-1} . The sharp spectral peak at wavenumber 842 cm^{-1}
 276 attributes to the peak of internal- CH_2 group [36]. C-H bond vibration and C-O-C of ether is indicated
 277 at wavenumber 949 cm^{-1} [37] and 1105 cm^{-1} [38] respectively. And the small sharp peaks between
 278 $1230\text{-}1350\text{ cm}^{-1}$ attributes to C-H scissor & bending vibration [39]. Absorption spectral peak at 2880
 279 cm^{-1} attributes to C-H stretching vibration [40] and the wider peak around wavenumber 3448 cm^{-1}
 280 indicates the O-H stretching [39].

281 Given that both biochar and activated carbon are amorphous carbons with substantial
282 porosity, there is no real difference between them structurally. Even activated carbon made from
283 biomass can be classified as a specific kind of activated biochar. However, unlike activated carbon,
284 biochar usually has abundant surface functional groups (C–O, C=O, COOH, and OH, etc.), which
285 being highly modifiable act as a platform for the synthesis of various functionalized carbon materials
286 [41]. However, the currently synthesized coconut shell biochar nanomaterial is not modified based
287 on functionalization elements and are developed without any further chemical processing.
288 Subsequently the surface functional groups C–O, C=O, COOH becomes inactive as the developed
289 biochar material has been synthesized using tube furnace at very high temperature of 1000 °C. During
290 this process, the functional groups are least active and becomes inert on investigation under FTIR in
291 the finger and functional group regions. The above inference is supported by the research work
292 presented by Elnour et al. [42] where biochar nanoparticles were developed via pyrolysis at different
293 temperature (300 °C, 400 °C, 500 °C, 600 °C and 700 °C), and disappearance of peaks are noticed.
294 Likewise, investigating CS nanoparticles under FTIR denotes no spectral spikes, indicating the
295 inactiveness of CS nanoparticles under the infrared spectrum. The nanocomposites of PEG with
296 different weight concentration of CS nanoparticles, replicates the absorption spectral peaks as
297 available in pure PEG-1000 PCM. Other than peak shifts, no spectral peaks seemed, thereby ensuring
298 the interaction between PEG and CS nanoparticles to be only physical and no chemical reaction
299 occurring between confirming the thermal stability. Subsequently XRD analysis of nanomaterial,
300 PCM and nanocomposites are provided in (Supplementary S8).



301

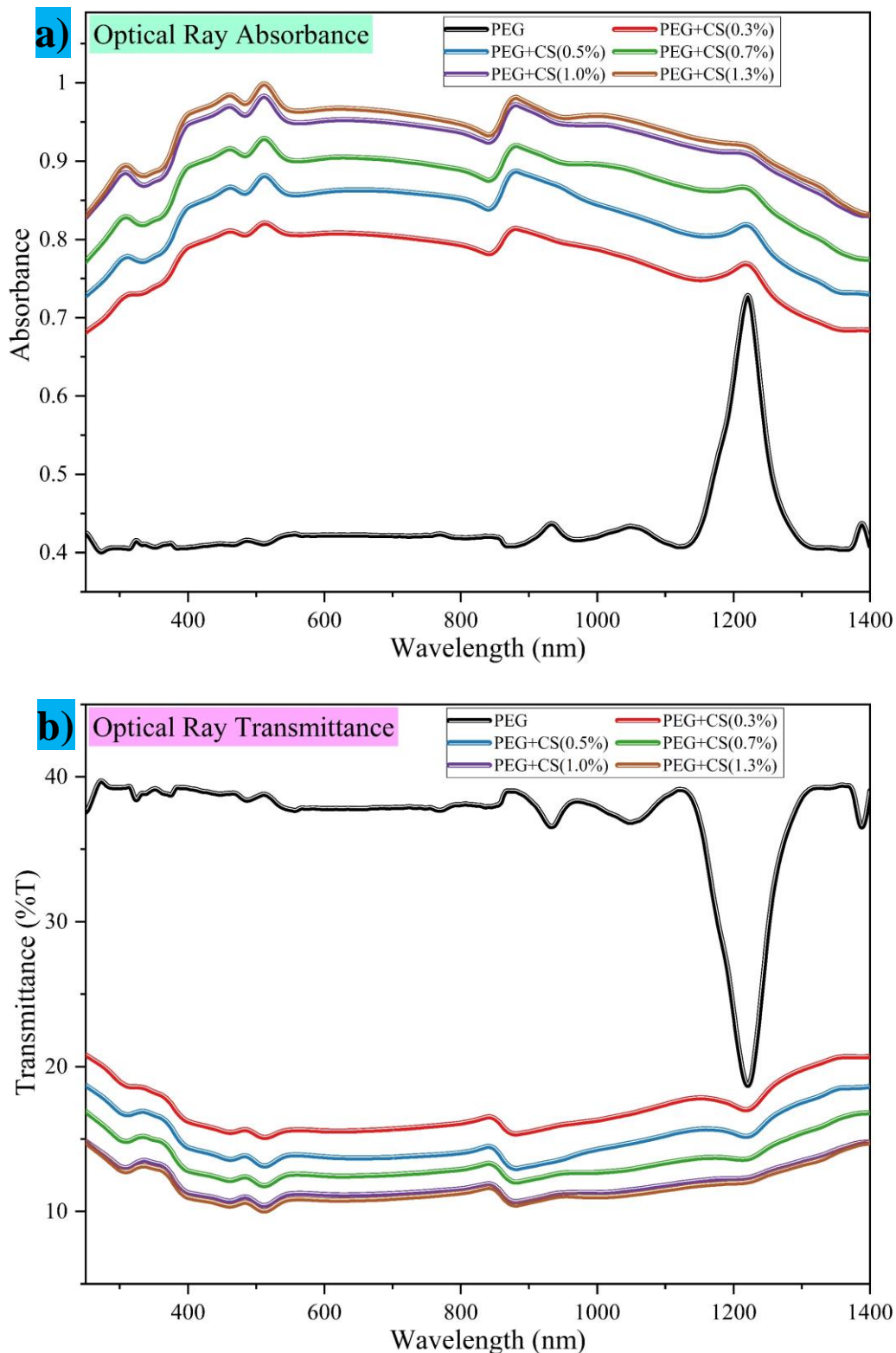
302 *Figure 3: Function group and chemical stability analysis of base PCM and its nanocomposite with*
303 *CS nanoparticle.*

304 **3.3 Optical absorbance and transmittance analysis**

305 In this section, the optical properties like absorption and transmittance of PEG-1000 PCM
306 and its nanocomposite with CS nanoparticle on incidence of photon within the electromagnetic
307 radiation spectrum is investigated. Figure 4a & 4b illustrates the optical absorption and optical
308 transmittance spectrum curve of PEG-1000 and the nanocomposite of CS nanoparticle dispersed
309 PCM at different weight fraction. A beam of light rays is passed on PCM nanocomposite samples to
310 understand the atoms and molecules absorbance potential exciting themselves from lower orbitals to
311 higher orbitals. Phase change materials are thermal energy storage materials acting as thermal
312 batteries. Meanwhile, the predominant source of eco-friendly thermal energy source is solar, radiating
313 thermal energy in the form of electromagnetic waves. Henceforth, it is vital to evaluate and
314 understand the optical properties of PCM for efficient development and integration of PCM with
315 advanced technologies. From Figure 4a, the optical electromagnetic ray absorbance of PEG-1000 is
316 inferred to be 0.43 owing to the opaque nature of organic material, and transparent texture of
317 polyethylene glycol. Meanwhile with different weight concentrations of CS nanoparticles, there is an
318 increasing trend. A CS nanoparticle with weight fraction of 0.3 wt%, 0.5 wt%, 0.7 wt%, 1.0 wt% and
319 1.3 wt% exhibits an optical absorbance of 0.77, 0.83, 0.87, 0.92 and 0.94 respectively. A maximum
320 increment in optical absorbance of about 118.6% is observed in the developed nanocomposite PCM
321 with 1.3 wt% of CS nanoparticle. Increase in optical absorption of electromagnetic rays by PEG-
322 1000 on dispersion of CS nanoparticles can be attributed to the following reasons; a) inclusion of CS
323 nanoparticle reduces the band gap of the organic PCM molecules and improves n-electrons, π -
324 electrons or combination of n-electrons & π -electrons to absorb the incidence radiation to excite the
325 electrons more actively to the higher orbitals [43]; b) likewise the dark texture of CS nanoparticle,
326 on uniform dispersion within the matrix of PCM contributes for better absorbance [8]. In addition the
327 porous frame like structure of the CS nanoparticle, supports multiple reflection within the
328 nanocomposite to better retrain the incident rays [44].

329 Similarly, the transmissibility of PEG-1000 and its nanocomposite with CS nanoparticle is
330 calculated by comparing the spectral curves with the extra-terrestrial spectrum data [45]. On
331 evaluation, PEG-1000 PCM exhibits an optical transmittance of 37.7%. Meanwhile, the
332 transmissibility of the developed nanocomposite of PEG with CS nanoparticles at weight fraction of
333 0.3 wt%, 0.5 wt%, 0.7 wt%, 1.0 wt% and 1.3 wt% is calculated to be 16.3%, 14.4%, 12.9%, 11.5%
334 and 11.2% respectively. As the experiment is conducted within a closed environment, the reflection
335 is negligible and the predominant phenomena of the incidence radiation is either absorption or

336 transmittance. As absorption and transmittance of electromagnetic rays are inversely proportional,
337 increase in absorbance leads to decrease in transmissible nature of organic PEG. This optical
338 absorbance property of the developed nanocomposite PCM sample is an excellent candidate for
339 integration of PCM with solar thermal systems.



340
341 *Figure 04: a) Optical Absorbance and b) Optical Transmittance of green synthesised coconut shell*
342 *nanoparticle dispersed PEG-1000 nanocomposites*

343
344
345
346
347
348
349
350
351
352
353
354
355
356
357
358
359
360
361
362

363
364
365
366
367
368
369
370
371
372
373

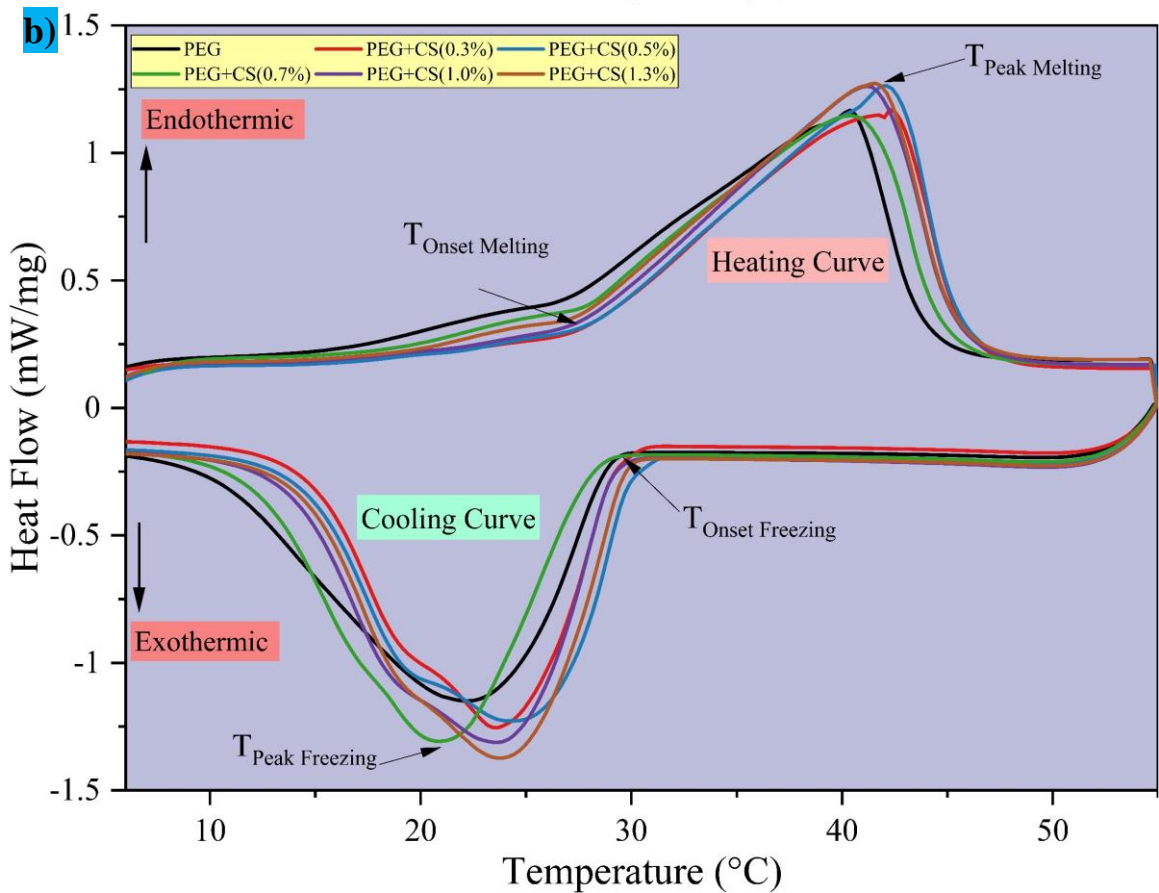
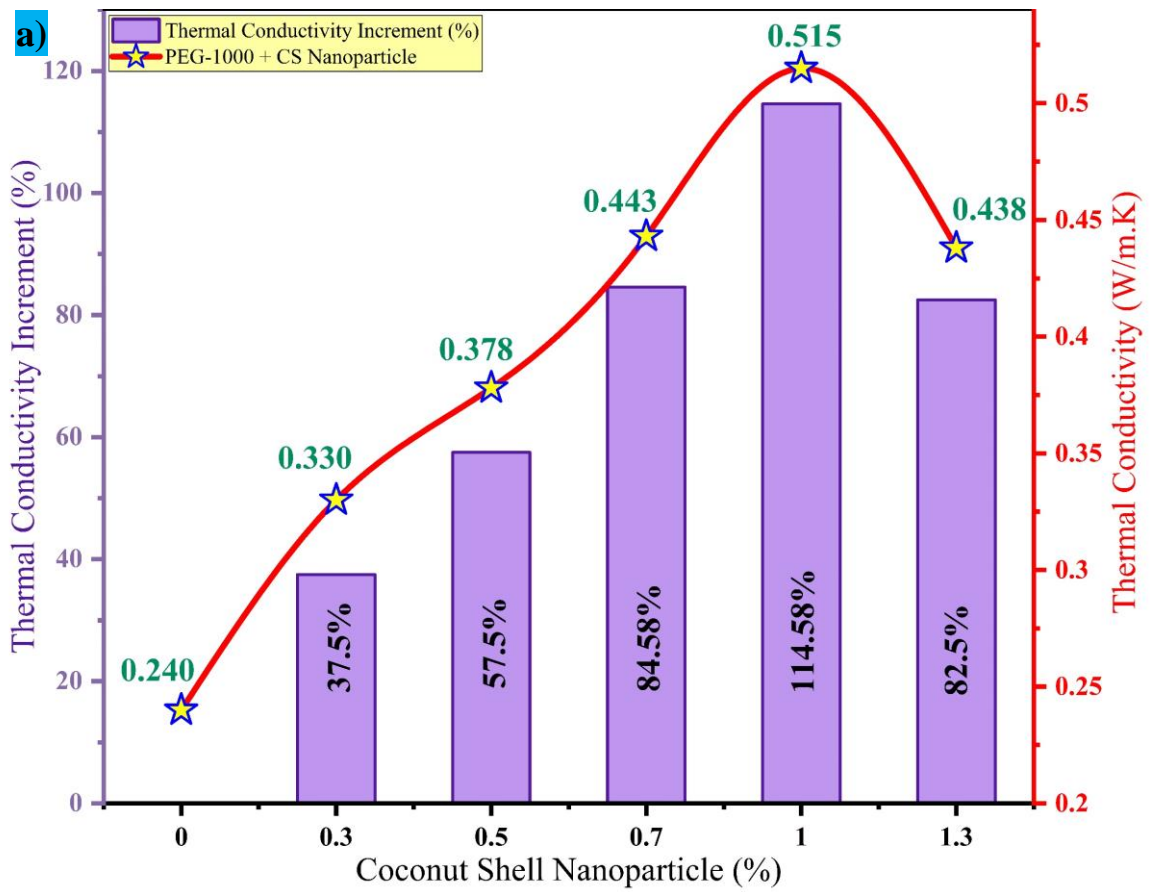
374

375

3.4 Thermal conductivity

Amidst the thermal features like, energy storage potential and thermal stability, thermal conductivity is a critical factor influencing the heat transfer rate or thermal response rate of energy storage materials. Thermal conductivity of PCM and its nanocomposite with CS nanoparticles are displayed in Figure 5a. In solid state, the thermal conductivity of PEG-1000 is measured to be 0.240 W/m·K signifying the low thermal energy charging/discharging efficiency. Nonetheless, developed nanocomposite samples of PEG with CS nanoparticle at weight fraction of 0.3 wt%, 0.5 wt%, 0.7 wt%, 1.0 wt% and 1.3 wt% depicts thermal conductivity of 0.330 W/m·K, 0.378 W/m·K, 0.443 W/m·K, 0.515 W/m·K and 0.438 W/m·K respectively. Thermal conductivity of PEG is increased 2.14 times using the green synthesised CS nanoparticle through a two-step process. The direct instigation behind this thermal conductivity increment are; a) uninterrupted three-dimensional network & porous structure established better contact area with PEG, causing low interfacial thermal resistance for improved thermal network channels and pathways for extra heat transfer and phonon propagation in PEG+CS nano composite samples [46]; b) uniform dispersion of high conducting CS nanoparticle develops thermal networks within the matrix of organic PCM for improved heat transfer. In addition, the green synthesised CS nanoparticle consists of 92% of carbon element as inferred from elemental analysis depicting the thermal conductivity of the CS nanoparticle to be in the range of 116-160 W/m·K [47]. CS nanoparticle, creates numerous thermal hotspots among the matrix of PEG-1000 and contributes towards better thermal networks for effective energy transfer rate of the developed nano composite [48].

In contrast it is observed that at higher concentration of 1.3 wt% CS nanoparticles with PEG organic PCM, significant drop in thermal conductivity of the nanocomposite is noted, which is worthy of discussion. At higher concentration the following phenomena occurs a) the cohesive force of attraction between the CS nanoparticle tends to increase causing formation of clusters, this clusters slowly bulge to become dense molecule and due to agglomeration settles down on repeated phase transition and disrupts the uniform distribution for proper thermal channel [49] and b) the mean free path for intermolecular diffusion is restricted due to increase in density of the composite PCM. Additionally, to compare the thermal feature like thermal conductivity and energy storage of PEG/CS nanocomposite with other porous carbon-based three dimensional nanoparticles in existing literatures are consolidate in Table 1, which demonstrates the superior thermal properties of the developed nanocomposite in justification to the novelty of the current research.



376
 377 *Figure 05: Thermo physical properties a) thermal conductivity increment of PEG-1000 PCM at*
 378 *different weight fraction of CS nanoparticle; b) Heating and Cooling Curve of nanocomposite PCM*
 379 *to analysis the heat storage enthalpy*

380 3.5 Energy storage ability

381 Phase change thermal properties like melting (ΔH_m) and cooling (ΔH_c) enthalpy, phase
382 transition temperature (T_m) of the developed CS nanoparticle dispersed nanocomposite PCMs, were
383 studied using DSC instrument. The heat flow curves of PEG-1000 and PEG+CS nanoparticles at
384 different weight fraction during phase transition process are depicted in Figure 5b. Enthalpy of the
385 developed CS biochar based nanocomposite PCM during heating at weight fraction of 0.3 wt%, 0.5
386 wt%, 0.7 wt%, 1.0 wt% and 1.3 wt% are 143.5 J/g, 148.2 J/g, 149.2 J/g, 150.1 J/g and 153.1 J/g
387 respectively whereas for base PEG-1000 PCM the heating enthalpy is only 141.2 J/g. Whereas during
388 freezing process, nanocomposite PCMs with 0.3 wt%, 0.5 wt%, 0.7 wt%, 1.0 wt% and 1.3 wt%
389 weight fraction of CS nanomaterial exhibit crystallization enthalpy of 138.9 J/g, 139.5 J/g, 140.7 J/g,
390 141.4 J/g and 146.3 J/g respectively whereas for base PEG-1000 PCM the crystallization enthalpy is
391 only 138 J/g. The DSC heat flow curve contains a single peak in both endothermic and exothermic
392 processes indicating the solid liquid phase transition. There is small drift in the melting temperature
393 of PEG with increased weight fraction of CS nanoparticles in the direction of higher temperature
394 compared to pure PEG. Likewise, the crystallisation temperature of the nanocomposite samples
395 shows an advance in freezing. The change in phase transition temperature of the nanocomposite can
396 be ascribed due to the porous structure nanoparticle effectively bonding the PCM and shifts the
397 temperature slightly.

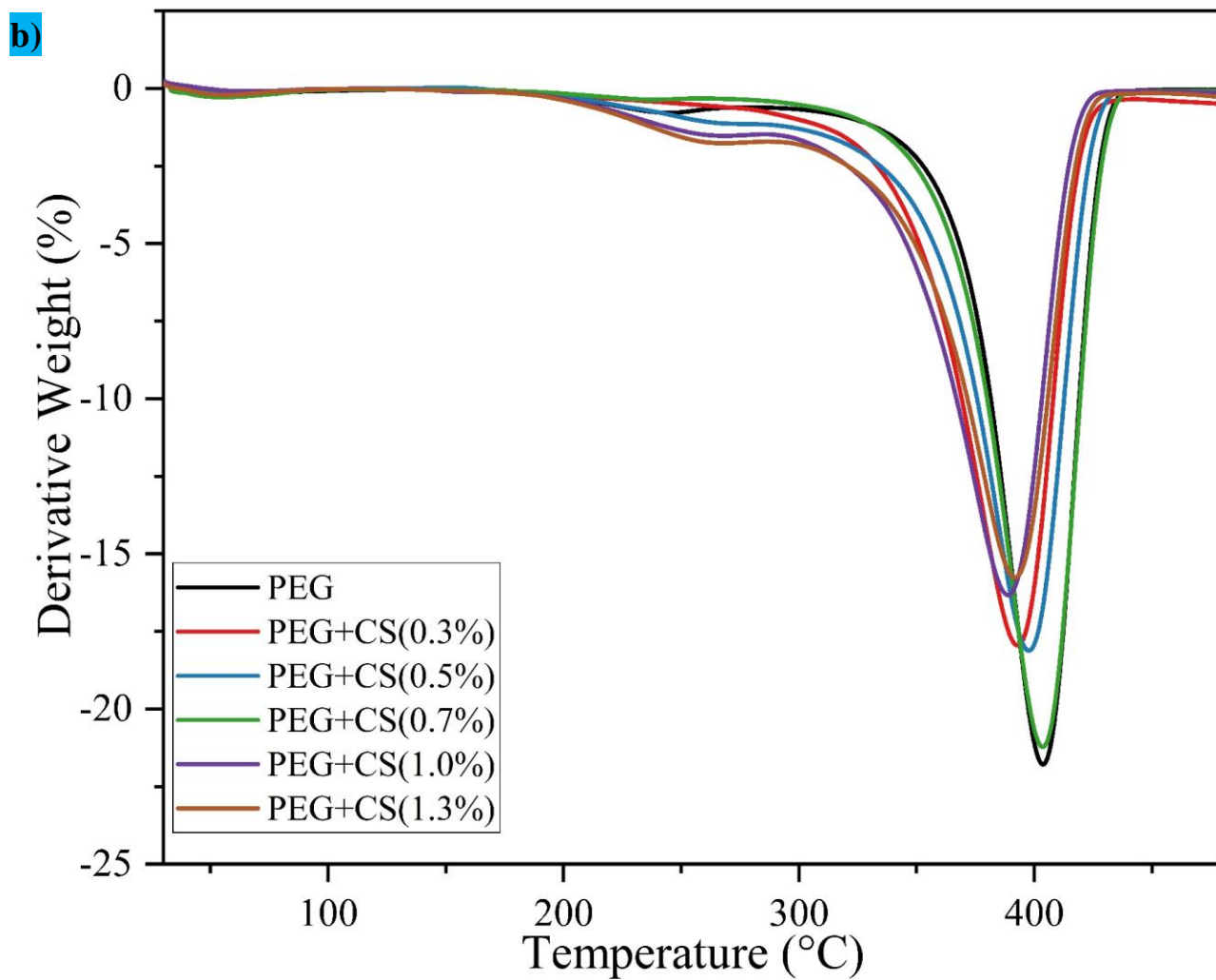
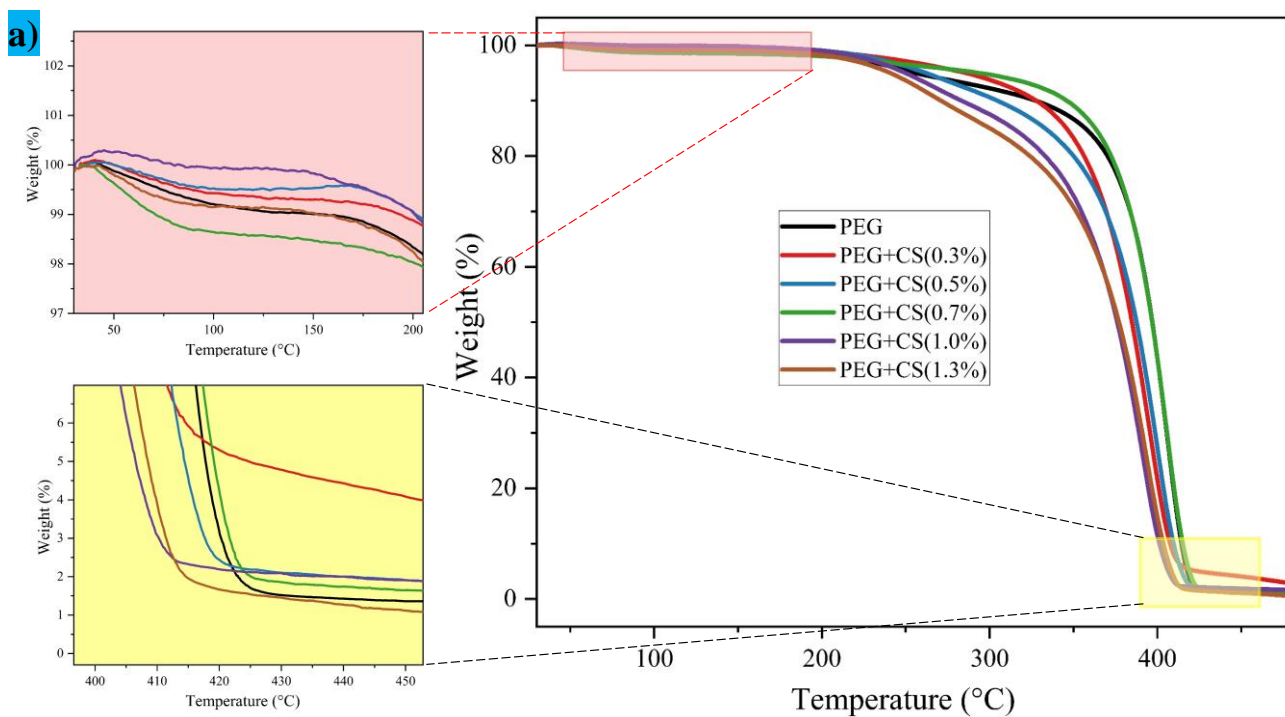
398 Furthermore, by analysing the area under the melting and cooling curve the phase transition
399 is calculated. Apparently, the PCM pure PEG-1000 is an exceptional candidate for storing thermal
400 energy owing to its latent heat of 142 J/g with phase transition temperature of 35-40 °C. Likewise
401 PEG+CS nanocomposite exhibit a potential for cyclic heat storage/release ability at the same
402 temperature range. On evaluation it is observed that the dispersed CS nanoparticles shows an
403 increasing trend in melting enthalpy of the developed nanocomposite sample, which can be attributed
404 due to a) the presence of C-H bond in the PEG+CS nanocomposite and higher number of domain
405 electrons on the surface of nanoparticle affects and the intermolecular bonding between the interface
406 of PEG and CS nanoparticle. The intermolecular force of attraction increases as PEG gets embedded
407 within the porous gaps of CS nanoparticles and ensures stability [9]. With low concentration of CS
408 nanoparticle, the strong intermolecular attraction is predominant and the melting enthalpy increases.
409 Whereas at higher concentration of nanoparticles the replacement of energy storage PCM is
410 maximum, and the increment occurring with intermolecular force of attraction becomes negligible
411 results in lower melting enthalpy.

412

413 3.6 Thermal degradation evaluation

414 Thermogravimetric analysis (TGA) is used to evaluate the thermal stability and thermal
415 degradation of PEG and its nanocomposites with CS nanoparticles. All the samples were heated to
416 500 °C at the rate of 10 °C/min under N₂ atmospheres using the TGA instrument to express better
417 understanding of their thermal stability and thermal degradation nature. TGA and DTG thermal
418 curves of PEG and PEG+CS nanocomposites are shown in Figure 6. It can be inferred from the TGA
419 curve that PEG and its nanocomposite undergo a single step degradation. Until 215 °C, the developed
420 nanocomposite samples exhibit extreme thermal stability and weight loss is negligible, whereas on
421 further increase in temperature, PEG and its nanocomposites starts to degrade with infinitesimal
422 variation in temperature. PEG decompose about 94% between the temperature ranges of 220-400 °C
423 as the long chain polymer in PEG breaks down into monomer during heating at higher temperature,
424 and the decomposition occurs [43]. The degradation of PEG reaches maximum weight percentage at
425 405 °C and the degradation process is completed at 440 °C. Moreover, the initial decomposition of
426 PEG+CS(1.0%) occurs at higher temperature than pure PEG, ensuring that PEG+CS(1.0) sample
427 exhibit outstanding thermal stability. Conversely, PEG+CS(1.0%) display early decomposition ahead
428 of pure PEG, which is owing to the micro-composite formation between CS nanoparticle and PCM
429 due to breakdown of molecules at higher temperature [50].

430 Differential thermogravimetric (DTG) curve of PEG and its nanocomposite with CS
431 nanoparticle in Figure 6b depicts the derivative weight loss, which reflects the concentration of
432 nanoparticles in the developed composite. Owing to high purity PEG undergoes maximum weight
433 loss during decomposition, whereas other composites lose lower percentage of weight compared to
434 pure PEG. The shift in final degradation temperature of the nanocomposite samples can be better
435 interpreted from the DTG curve. However, the working temperature for the developed nano
436 composite is usually below 55 °C as its phase transition temperature is 38 °C, which is far lower than
437 the degradation temperature of the tested samples, and is preferred for thermal regulation systems.
438 More information on the TGA analysis of the developed nanocomposite can be inferred from visuals
439 presented ([Supplementary S9-S14 and Appendix V](#))



440
 441 *Figure 06: a) Thermal degradation curve and b) differential thermogravimetric (DTG) curve of PEG-*
 442 *1000 and its nanocomposites with CS nanoparticles.*

443

3.7 Thermal cycling potential

444

445

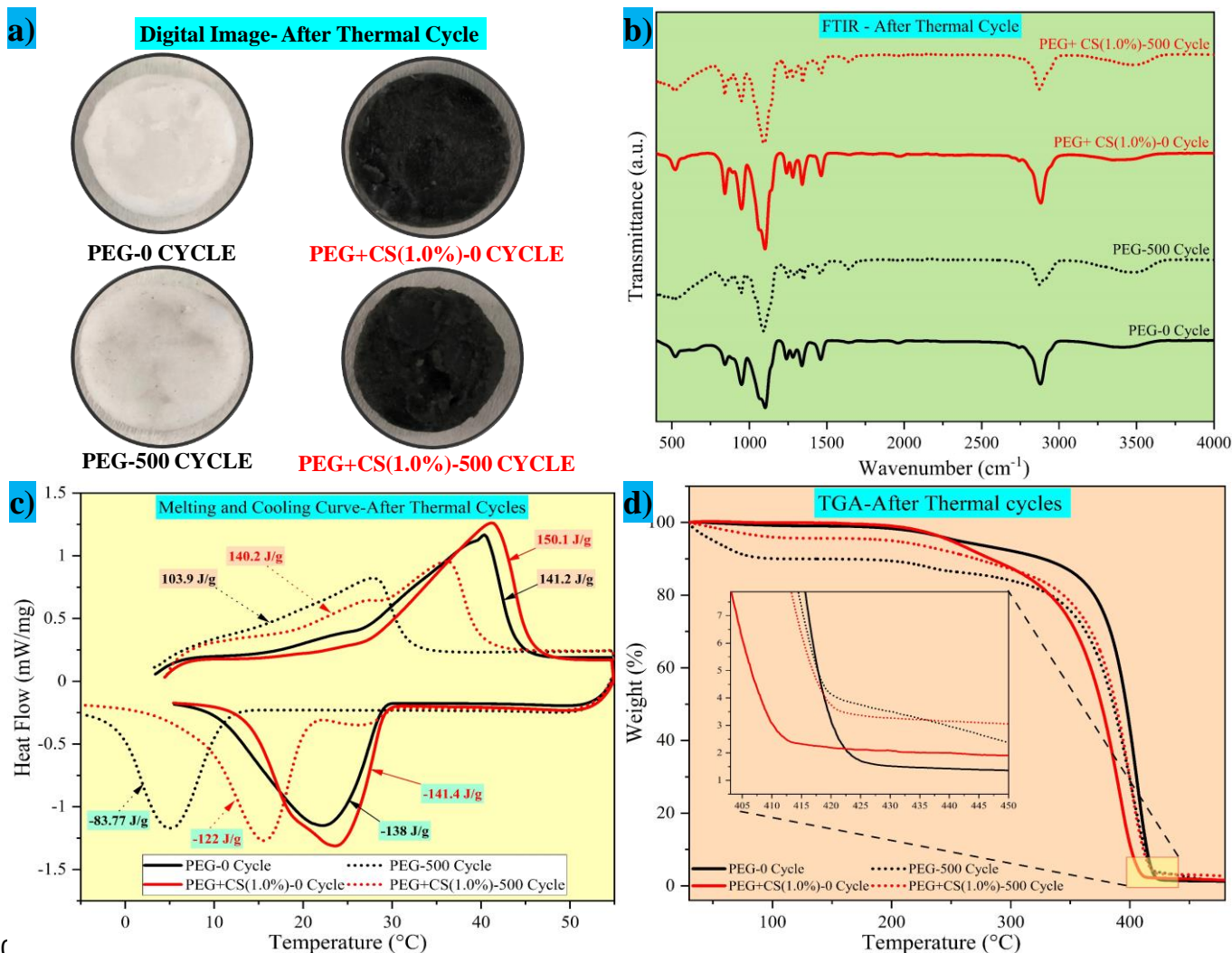
446

447

448

449

Thermal stability and reusability potential of the developed nanocomposite PCMs is a crucial feature, which restricts their integration with real time thermal systems. Herein, we investigate the thermal stability of PEG/CS nanocomposite PCM with 1.0 wt% of CS nanoparticles for 500 numbers of charging and discharging thermal cycles. Figure 7 consolidates the chemical stability evaluation by FTIR spectrum, energy storage heat flow curves and thermogravimetric curve of PEG and PEG/CS nanocomposite PCM before and after 500 cycles.



450

451

452

453

Figure 07: Evaluation of PEG and PEG/CS nanocomposite before and after 500 thermal cycles a) Digital image; b) Chemical stability using FTIR; c) Energy storage potential and d) Thermal degradation curve.

454

455

456

457

458

The digital view of PEG after 500 thermal cycles indicates change in texture and formation of carbon content with repeated thermal cycle, whereas PEG/CS nanocomposite does not exhibit much variation in texture. However, there is a change in the solidity of PEG and PEG/CS nanocomposite, which is a representation of weaker bonding of long chain polymers. Minor variation in FTIR spectrum can be noticed in Figure 7b, on comparison of PEG and PEG/CS samples before

459 and after thermal cycle, in regard to the intensity of the peak. Variation in intensity of peak is expected
460 as this is a common phenomenon owing to accelerated thermal cycle, whereas the peaks are in
461 correspondence to the same wavenumber before and after 500 thermal cycle. Conversely, no new
462 peaks are observed ensuring that no chemical reaction and thermal degradation has occurred with
463 repeated usage of PCM. Besides Figure 7c illustrates the heat flow curves of PEG and PEG/CS
464 nanocomposite with single peak ensuring the solid-liquid phase transition. As can be inferred from
465 above figure, the peak melting temperature of the PEG PCM is predominantly varied establishing a
466 instability during phase transition as its exposed higher temperature at a faster rate, and ageing of
467 PEG PCM occurs. Whereas with nanocomposite PEG+1.0CS, proper dispersion of CS nanoparticles
468 retains and absorbs much of heat supplied, and restricts breakage of intermolecular bonding between
469 PEG molecules and well facilitates CS nanoparticles binds stronger with PEG as they retain PCM
470 within their porous honeycomb structure and reduce the drop in melting temperature of PEG+CS
471 nanocomposite considerably. The variation in peak transition temperature of PEG/CS(1.0%) is far
472 within the margin of error providing extended operation of PCM for energy storage. Likewise, with
473 repeated thermal cycling's, the intermolecular force of attraction and the binding between the PEG-
474 PEG molecules and PEG-CS molecules disrupts and lowers the energy storage ability [28].
475 Furthermore, influence of impurity is also a factor to be considered causing reduction in energy
476 storage potential of the samples. Nonetheless, in real time application, the PCM are expected to
477 encapsulate within closed environment (preventing impurity), as well the operation temperature is
478 within permissible limit and the charging and discharging occurs at slow rate. In regard to the energy
479 storage potential (ΔH_m) and (ΔH_c) of PEG declines by 26.4% and 39.3% respectively after 500
480 thermal cycles, whereas (ΔH_m) and (ΔH_c) of PEG/CS(1.0%) shows a variation by 6.6% and 13.7%
481 after 500 number of thermal cycles. The heat flow results proves the ability of PEG/CS nanoparticles
482 to be opted for repeated usage within a drop in latent heat. During repeated thermal cycles, the
483 bonding between the long chain polymers weakens resulting in lower intermolecular force of
484 attraction reducing the energy storage enthalpy. Thermal conductivity of the developed
485 nanocomposite PCM after thermal cycling displays 0.501 W/m·K The drop in thermal conductivity
486 of the sample after 500 thermal cycles is owing to thermal cycling effect, where the developed
487 nanocomposite undergoes repeated energy storage and discharge. As we have conducted accelerated
488 thermal cycling of 500 thermal cycles, during the process inclusion of any impurities in the
489 environment is also more likely to impact the thermal conductivity. Another significant property
490 evaluated to ensure the ability of PCM for practical application is the thermal stability, which is
491 generally characterised using the thermogravimetric curve indicated in Figure 7d. Both PEG and
492 PEG/CS nanocomposite undergo one step thermal degradation before and after thermal cycling. It

493 can be inferred from the TGA curve, that PEG undergoes weight loss up to 10% within the
494 temperature range of 30-100°C, whereas PEG/CS nanocomposite depicts better thermal stability with
495 3-4% weight loss. Nonetheless, the maximum degradation temperature of pure PEG and its
496 nanocomposite with CS nanoparticles is increased after thermal cycling, which can be ascribed due
497 to the repeated heating and cooling. Thermal stability of PEG/CS(1.0%) nanocomposite exhibits
498 closely similar chemical and thermal stability before and after thermal cycling ensuring their potential
499 to be used in energy storage systems.

500 **4.0 Conclusion**

501 Novel three dimensional highly porous carbon based coconut shell nanoparticles are
502 successfully synthesised through green approach to be incorporated with PEG based PCMs adopting
503 two step methods to enhance the thermo physical features. CS nanoparticles with porous frame like
504 structure, supports multiple reflection of the incident electromagnetic waves within the **PCM matrix**
505 **and increases the optical absorbance from 0.43 to 0.94 contributing to about 118.6%. Subsequently,**
506 **the increase in optical absorbance reduces the transmittance of electromagnetic waves from 37.7% to**
507 **11.2%. PEG/CS nanocomposite PCM, specifically with weight fraction 1.0% possessed 3D thermal**
508 **conducting network resulting in thermal conductivity enhancement by 114.5% (from 0.24 W/m·K to**
509 **0.515 W/m·K). Conversely, they also demonstrate an increase in energy storage potential of 150.2**
510 **J/g compared to 141.2 J/g of PEG during heating and exhibits 141.4 J/g compared to 138 J/g of PEG**
511 **during freezing.** More importantly, the developed nanocomposite maintains the thermal feature even
512 after 500 thermal cycles, ensuring their charging and discharging potential for reusability. Possessing,
513 excellent chemical stability, optical absorbance, thermal feature like thermal response, energy storage
514 and thermal stability brands the developed CS nanoparticle dispersed PEG/CS nano composite PCMs
515 to be envisaged in low temperature waste heat recovery, thermoregulation comfort in buildings,
516 electronic cooling system, and so on.

517 **Acknowledgement**

518 Authors acknowledges the financial assistance of Sunway University through Sunway University's
519 International Research Network Grant Scheme 2.0 (IRNGS 2.0) 2022 (STR-IRNGS-SET-RCNMET-
520 01-2021) for carrying out this research. The authors are thankful to the Deanship of Scientific
521 Research at Najran University for funding this work under the Research Groups Funding program
522 grant code (NU/RG/SERC/11/7)

523

524 **Reference**

- 525 1. Wu, S., et al., *High-performance thermally conductive phase change composites by large-size oriented*
526 *graphite sheets for scalable thermal energy harvesting*. *Advanced Materials*, 2019. **31**(49): p.
527 1905099.
- 528 2. Mehling, H. and L.F. Cabeza, *Phase change materials and their basic properties*, in *Thermal energy*
529 *storage for sustainable energy consumption: fundamentals, case studies and design*. 2007, Springer.
530 p. 257-277.
- 531 3. Gerkman, M.A. and G.G. Han, *Toward controlled thermal energy storage and release in organic*
532 *phase change materials*. *Joule*, 2020. **4**(8): p. 1621-1625.
- 533 4. Li, Z.-R., N. Hu, and L.-W. Fan, *Nanocomposite phase change materials for high-performance*
534 *thermal energy storage: A critical review*. *Energy Storage Materials*, 2022.
- 535 5. Kalidasan, B., et al., *Nano additive enhanced salt hydrate phase change materials for thermal energy*
536 *storage*. *International Materials Reviews*, 2023. **68**(2): p. 140-183.
- 537 6. Gao, D.-c., et al., *Mineral-based form-stable phase change materials for thermal energy storage: A*
538 *state-of-the art review*. *Energy Storage Materials*, 2022. **46**: p. 100-128.
- 539 7. Kumar, R., et al., *A comparative study on thermophysical properties of functionalized and non-*
540 *functionalized Multi-Walled Carbon Nano Tubes (MWCNTs) enhanced salt hydrate phase change*
541 *material*. *Solar Energy Materials and Solar Cells*, 2022. **240**: p. 111697.
- 542 8. Kumar, R., et al., *Investigation of thermal performance and chemical stability of graphene enhanced*
543 *phase change material for thermal energy storage*. *Physics and Chemistry of the Earth, Parts A/B/C*,
544 2022. **128**: p. 103250.
- 545 9. Kalidasan, B., et al., *Synthesis and characterization of conducting Polyaniline@ cobalt-Paraffin wax*
546 *nanocomposite as nano-phase change material: Enhanced thermophysical properties*. *Renewable*
547 *Energy*, 2021. **173**: p. 1057-1069.
- 548 10. Balasubramanian, K., et al., *Tetrapods based engineering of organic phase change material for*
549 *thermal energy storage*. *Chemical Engineering Journal*, 2023. **462**: p. 141984.
- 550 11. Paneliya, S., et al., *Core shell paraffin/silica nanocomposite: A promising phase change material for*
551 *thermal energy storage*. *Renewable Energy*, 2021. **167**: p. 591-599.
- 552 12. Sun, J., et al., *Composites with a novel core-shell structural expanded perlite/polyethylene glycol*
553 *composite PCM as novel green energy storage composites for building energy conservation*. *Applied*
554 *Energy*, 2023. **330**: p. 120363.
- 555 13. Zhu, X., et al., *Facile synthesis of hierarchical porous carbon material by potassium tartrate*
556 *activation for chloramphenicol removal*. *Journal of the Taiwan Institute of Chemical Engineers*, 2018.
557 **85**: p. 141-148.
- 558 14. Dawood, S., T.K. Sen, and C. Phan, *Synthesis and characterization of slow pyrolysis pine cone bio-*
559 *char in the removal of organic and inorganic pollutants from aqueous solution by adsorption: kinetic,*
560 *equilibrium, mechanism and thermodynamic*. *Bioresource Technology*, 2017. **246**: p. 76-81.
- 561 15. Hagemann, N., et al., *Activated carbon, biochar and charcoal: linkages and synergies across*
562 *pyrogenic carbon's ABC s*. *Water*, 2018. **10**(2): p. 182.
- 563 16. Magnacca, G., et al., *Preparation, characterization and environmental/electrochemical energy*
564 *storage testing of low-cost biochar from natural chitin obtained via pyrolysis at mild conditions*.
565 *Applied Surface Science*, 2018. **427**: p. 883-893.
- 566 17. Soffian, M.S., et al., *Carbon-based material derived from biomass waste for wastewater treatment*.
567 *Environmental Advances*, 2022. **9**: p. 100259.
- 568 18. Sheng, N., et al., *Honeycomb carbon fibers strengthened composite phase change materials for*
569 *superior thermal energy storage*. *Applied Thermal Engineering*, 2020. **164**: p. 114493.
- 570 19. Das, D., et al., *A novel form stable PCM based bio composite material for solar thermal energy storage*
571 *applications*. *Journal of Energy Storage*, 2020. **30**: p. 101403.
- 572 20. Xiong, T., et al., *Preparation and thermal conductivity enhancement of a paraffin wax-based*
573 *composite phase change material doped with garlic stem biochar microparticles*. *Science of the Total*
574 *Environment*, 2022. **827**: p. 154341.
- 575 21. Lv, L., et al., *Effect of structural characteristics and surface functional groups of biochar on thermal*
576 *properties of different organic phase change materials: Dominant encapsulation mechanisms*.
577 *Renewable Energy*, 2022. **195**: p. 1238-1252.

- 578 22. Wan, Y.-c., et al., *A promising form-stable phase change material prepared using cost effective*
579 *pinecone biochar as the matrix of palmitic acid for thermal energy storage*. Scientific Reports, 2019.
580 **9**(1): p. 11535.
- 581 23. Mandal, S., et al., *Optimization of eco-friendly Pinus resinosa biochar-dodecanoic acid phase change*
582 *composite for the cleaner environment*. Journal of Energy Storage, 2022. **55**: p. 105414.
- 583 24. Chen, W., et al., *Effect of GO on the Structure and Properties of PEG/Biochar Phase Change*
584 *Composites*. Polymers, 2023. **15**(4): p. 963.
- 585 25. Atinafu, D.G., et al., *Engineering biochar with multiwalled carbon nanotube for efficient phase*
586 *change material encapsulation and thermal energy storage*. Energy, 2021. **216**: p. 119294.
- 587 26. Goud, M. and F. Raval, *A sustainable biochar-based shape stable composite phase change material*
588 *for thermal management of a lithium-ion battery system and hybrid neural network modeling for heat*
589 *flow prediction*. Journal of Energy Storage, 2022. **56**: p. 106163.
- 590 27. Bordoloi, U., et al., *Synthesis and comparative analysis of biochar based form-stable phase change*
591 *materials for thermal management of buildings*. Journal of Energy Storage, 2022. **55**: p. 105801.
- 592 28. Kalidasan, B., et al., *Eco-friendly coconut shell biochar based nano-inclusion for sustainable energy*
593 *storage of binary eutectic salt hydrate phase change materials*. Solar Energy Materials and Solar
594 Cells, 2023. **262**: p. 112534.
- 595 29. Zhang, X., et al., *Thermal conductivity enhancement of polyethylene glycol/expanded perlite with*
596 *carbon layer for heat storage application*. Energy and Buildings, 2016. **130**: p. 113-121.
- 597 30. Karaman, S., et al., *Polyethylene glycol (PEG)/diatomite composite as a novel form-stable phase*
598 *change material for thermal energy storage*. Solar Energy Materials and Solar Cells, 2011. **95**(7): p.
599 1647-1653.
- 600 31. Deng, Y., et al., *Thermal conductivity enhancement of polyethylene glycol/expanded vermiculite*
601 *shape-stabilized composite phase change materials with silver nanowire for thermal energy storage*.
602 Chemical Engineering Journal, 2016. **295**: p. 427-435.
- 603 32. Khanna, S., et al., *Investigating the thermal properties of n-hexacosane/graphene composite: A highly*
604 *stable nanocomposite material for energy storage application*. Thermal Science and Engineering
605 Progress, 2023. **39**: p. 101712.
- 606 33. Kuziel, A.W., et al., *Ultra-long carbon nanotube-paraffin composites of record thermal conductivity*
607 *and high phase change enthalpy among paraffin-based heat storage materials*. Journal of Energy
608 Storage, 2021. **36**: p. 102396.
- 609 34. Cheng, G., X. Wang, and Y. He, *3D graphene paraffin composites based on sponge skeleton for photo*
610 *thermal conversion and energy storage*. Applied Thermal Engineering, 2020. **178**: p. 115560.
- 611 35. Khanna, S., et al., *Ultra-stable silica/exfoliated graphite encapsulated n-hexacosane phase change*
612 *nanocomposite: A promising material for thermal energy storage applications*. Energy, 2022. **250**: p.
613 123729.
- 614 36. Shi, J. and M. Li, *Synthesis and characterization of polyethylene glycol/modified attapulgite form-*
615 *stable composite phase change material for thermal energy storage*. Solar Energy, 2020. **205**: p. 62-
616 73.
- 617 37. Peng, L., et al., *New energy-saving building developed by using polyethylene glycol/halloysite*
618 *nanotube energy-storage blanket and heat-insulating glass with Na_xWO₃@ SiO₂ nano-coating*. Solar
619 Energy Materials and Solar Cells, 2023. **250**: p. 112074.
- 620 38. Wang, C., et al., *Thermal behavior of polyethylene glycol based phase change materials for thermal*
621 *energy storage with multiwall carbon nanotubes additives*. Energy, 2019. **180**: p. 873-880.
- 622 39. Wang, T., et al., *Electro-and photo-thermal energy conversion investigation of polyethylene glycol*
623 *infiltrated porous carbon aerogels*. Journal of Energy Storage, 2023. **68**: p. 107724.
- 624 40. Li, Y., et al., *Processing wood into a phase change material with high solar-thermal conversion*
625 *efficiency by introducing stable polyethylene glycol-based energy storage polymer*. Energy, 2022.
626 **254**: p. 124206.
- 627 41. Liu, W.-J., H. Jiang, and H.-Q. Yu, *Development of biochar-based functional materials: toward a*
628 *sustainable platform carbon material*. Chemical reviews, 2015. **115**(22): p. 12251-12285.
- 629 42. Elnour, A.Y., et al., *Effect of pyrolysis temperature on biochar microstructural evolution,*
630 *physicochemical characteristics, and its influence on biochar/polypropylene composites*. Applied
631 sciences, 2019. **9**(6): p. 1149.
- 632 43. Balasubramanian, K., et al., *Tetrapods based Engineering of Organic Phase Change Material for*
633 *Thermal Energy Storage*. Chemical Engineering Journal, 2023: p. 141984.

- 634 44. Gao, H., et al., *Energy harvesting and storage blocks based on 3D oriented expanded graphite and*
635 *stearic acid with high thermal conductivity for solar thermal application*. *Energy*, 2022. **254**: p.
636 124198.
- 637 45. Gueymard, C.A., *The sun's total and spectral irradiance for solar energy applications and solar*
638 *radiation models*. *Solar energy*, 2004. **76**(4): p. 423-453.
- 639 46. Tong, X., et al., *Organic phase change materials confined in carbon-based materials for thermal*
640 *properties enhancement: Recent advancement and challenges*. *Renewable and Sustainable Energy*
641 *Reviews*, 2019. **108**: p. 398-422.
- 642 47. Muruges, M., *The elements of periodic table*. Heidelberg: Springer, 2019.
- 643 48. Kalidasan, B., et al., *Graphene–Silver Hybrid Nanoparticle based Organic Phase Change Materials*
644 *for Enhanced Thermal Energy Storage*. *Sustainability*, 2022. **14**(20): p. 13240.
- 645 49. Shen, Z., et al., *Enhanced thermal energy storage performance of salt hydrate phase change material:*
646 *effect of cellulose nanofibril and graphene nanoplatelet*. *Solar Energy Materials and Solar Cells*, 2021.
647 **225**: p. 111028.
- 648 50. Kalidasan, B., et al., *Energizing organic phase change materials using silver nanoparticles for*
649 *thermal energy storage*. *Journal of Energy Storage*, 2023. **58**: p. 106361.